Mesoscale Eddy - Internal Wave Coupling. III. The End of the Enstrophy Cascade and Implications for the Fast Manifold - Slow Manifold Debate

Kurt L. Polzin *

*Corresponding author address: Kurt L. Polzin, MS#21 WHOI Woods Hole MA, 02543.
E-mail: kpolzin@whoi.edu

Abstract

The issue of internal wave–mesoscale eddy interactions is revisited. Previous theoretical work identified the mesoscale eddy field as a possible source of internal wave energy and pseudomomentum. Adiabatic pseudomomentum flux divergences, in turn, serve as a sink of eddy potential vorticity and contribute to potential enstrophy (potential vorticity squared) dissipation.

A potential enstrophy budget for the Local Dynamics Experiment of the Poly-Mode field program is assessed using mesoscale eddy – internal wave coupling coefficients identified in a companion manuscript of $\nu_h \cong 50$ m^2 s^{-1} and $\nu_v + \frac{f^2}{N^2} K_h \cong 2.5 \times 10^{-3}$ m^2 s^{-1}. These estimates indicate that mesoscale eddy-internal wave interactions *may* play an $O(1)$ role in the mesoscale eddy potential enstrophy budget as enstrophy dissipation. This claim comes with significant caveats, however, as the Local Dynamics Experiment array data likely do not properly resolve the required spatial gradients of the mesoscale eddy field.

Previous radiation balance equation formulations for this coupling are examined. In these formulations *permanent* transfer of energy and internal wave pseudomomentum for mesoscale eddy potential vorticity is enabled by nonlinearity in the wavefield. Revision of these radiation balance equation formulations to account for non-local effects returns predictions of $\nu_h \cong 50 - 100$ m^2 s^{-1} and $\nu_v + \frac{f^2}{N^2} K_h \cong -0.008$ m^2 s^{-1}. The prediction for the effective vertical viscosity is very sensitive to how internal wave energy is distributed in the spectral domain. The difference between observed and predicted exchange coefficients is attributed to (i) differences between the observed internal wave spectrum and use of the Garrett and Munk model as a basis for the theoretical prediction and (ii) uncertainty in how to properly account for non-local effects in the model estimates.

In accounting for non-local effects, length scale dependent coupling coefficients can be derived. With such length scale dependent coupling coefficients, an argument is advanced that the estimates of enstrophy dissipation are biased *low* and thus the claim that mesoscale eddy-internal wave interactions *may* play an $O(1)$ role in the mesoscale eddy potential enstrophy budget as enstrophy dissipation is reinforced.

Finally, the process described here is best interpreted as an amplifier of a pre-existing or externally forced finite amplitude wavefield rather than the spontaneous imbalance of a linear field. Energy, pseudomomentum and vorticity can be transfered from the slow manifold (geostrophically balanced motions) to the fast manifold (internal gravity waves) via linear wave propagation in asymmetric background flows, but that transfer is reversible. The permanent transfer is accomplished by nonlinearity on the fast manifold.

1. Introduction

a. Preliminaries

Winds and air-sea exchanges of heat and fresh water are ultimately responsible for the basin-scale currents, or general circulation of the oceans. In order to achieve a state where the energy and enstrophy (vorticity squared) of the ocean is not continuously increasing, some form of dissipation is required to balance this forcing. While the above statement may seem obvious, little is known about how and where this dissipation occurs.

Early theories of the wind driven circulation [Stommel (1948), Munk (1950)] view the western boundary as a region where energy and vorticity input by winds in mid-gyre could be dissipated. Those theories predict Gulf Stream transports that are approximately equal to the interior Sverdrup transport [about 30 Sv, Schmitz et al. (1992)] and that are much smaller than observed Gulf Stream transports after the Stream separates from the coast [about 150 Sv, Johns et al. (1995)]. Subsequent theories of the wind driven circulation have attempted to address the role of nonlinearity and baroclinicity in increasing Gulf Stream transports above that given by the Sverdrup relation.

Hogg (1983) proposed the existence of two relatively barotropic recirculation gyres on either side of the Stream that combine to increase the total transport. It is now generally accepted that the recirculation gyres result from the 'absorption' of Planetary and Topographic Rossby Waves generated by the meandering of a baroclinicly unstable Gulf Stream. The 'absorption' process is uncertain and is a focus of this manuscript.

A cornerstone of theoretical understanding concerns zonal mean theory and the analysis of wave propagation in parallel shear flows. A basic constraint, typically referred to as Andrews and McIntyre's generalized Eliassen-Palm (EP) flux theorem:

$$\frac{d\, k\mathcal{A}}{dt} + \nabla \cdot \mathbf{F} = \mathcal{D} + O(\alpha^3); \tag{1}$$

states that in the absence of dissipation $\mathcal{D}$ and nonlinearity (small wave amplitude α limit), and for steady conditions, the Eliassen-Palm flux $\mathbf{F}$ is spatially nondivergent, $\nabla \cdot \mathbf{F} = 0$. In terms of either linear internal wave or linear Rossby wave kinematics, the Eliassen-Palm flux $\mathbf{F} = k\mathbf{C_g}\mathcal{A}$, with streamwise (zonal) wavenumber k, group velocity $\mathbf{C_g}$ and wave action $\mathcal{A}$. With respect to the mean fields, the attendant nonacceleration theorem (Andrews et al. 1987) states that the mean flow remains steady if $\nabla \cdot \mathbf{F} = 0$.

The Eliassen-Palm flux theorem thus sheds light upon the absorption process alluded to above as mean flows can be forced by the gamut of processes that balance the EP flux divergence. Hitherto, the oceanographic community has typically focused on the effects of nonlinearity within the mesoscale eddy field [Rhines and Schopp (1991); Jayne et al. (1996)].

The basics of nonlinearity for quasigeostrophic flows in the adiabatic and inviscid limits is the cascade of energy to larger scales and the cascade of potential enstrophy (potential vorticity squared) to smaller scales, [Rhines (1979); Salmon (1998)]. The potential enstrophy flux occurs without an energy flux so that the endpoint of the enstrophy cascade *could be* defined by molecular dissipation, or, perhaps more likely, by ambient turbulent processes unrelated to the enstrophy cascade. The energy budget *could be* closed by locating the energy sinks at the boundaries, i.e. in bottom Ekman layers and through eddy–mixed layer interactions. The potential enstrophy budget *could be* closed by mixing potential vorticity at a molecular level *without* attendant consequences for the energy budget. But is this true?

A second cornerstone of theoretical understanding is the material conservation of potential vorticity (Ertel 1942; Haynes and McIntyre 1987). In the absence of frictional and diabatic effects, potential vorticity is conserved following a fluid element. What constitutes friction, though, is not always obvious.

Despite the intellectual prejudice that views the oceanic interior as inviscid and adiabatic, or perhaps more precisely because, it seems prudent to quantify the rate at which interior processes damp both enstrophy and energy. A companion manuscript (Polzin 2009) examines the issue of energetics. Here I engage in an inquiry of how internal wave processes contribute as frictional effects and serve to mix eddy potential vorticity.

The companion work identifies coupling coefficients of $\nu_h \cong 50$ m^2 s^{-1} and $\nu_v + \frac{f^2}{N^2} K_h \cong 2.5 \times 10^{-3}$ m^2 s^{-1} from current meter data taken as part of the Local Dynamics Experiment (LDE) of the PolyMode field program. The purpose of this paper is to place those estimates into the LDE potential vorticity flux estimates of Brown et al. (1986) (Section 3). Theoretical estimates of the coupling are reviewed and revised in Section 4. Length scale dependence of the coupling coefficients and array resolution issues are covered in Section 5. A summary and discussion concludes the paper.

2. Groundwork

a. The coupling mechanism

The required tools from the companion manuscript are: (i) a Reynolds decomposition of the velocity [$\mathbf{u} = (u, v, w)$], buoyancy [$b = -g\rho/\rho_o$ with gravitational constant g and density ρ] and pressure [π] fields into a quasigeostrophic 'mean' ($\bar{}$) and small amplitude internal wave ($''$) perturbations on the basis of a time scale separation: $\psi = \overline{\psi} + \psi''$ with $\overline{\psi} = \tau^{-1} \int_0^\tau \psi \, dt$ in which τ is much longer than the internal wave time scale but smaller than the eddy time scale; (ii) a further assumption of a spatial scale separation in order to invoke the ray tracing limit of internal wave -mean flow interactions. In this limit the ray equations for the evolution of the wavevector $\mathbf{k} = (k, l, m)$ following a ray path,

$$\frac{d\mathbf{k}}{dt} = -\nabla(\omega + \mathbf{k} \cdot \overline{\mathbf{u}}) \tag{2}$$

have solutions $\mathbf{k} \propto e^{\pm(S_n^2 + S_s^2 - \zeta^2)^{1/2} t/2}$, in which $S_s \equiv \overline{v}_x + \overline{u}_y$ is the shear component of strain, $S_n \equiv \overline{u}_x - \overline{v}_y$ is the normal component, $\zeta \equiv \overline{v}_x - \overline{u}_y$ is relative vorticity and intrinsic frequency $\omega = \sigma - \mathbf{k} \cdot \overline{\mathbf{u}}$. Thus a wave packet in a quasigeostrophic eddy field undergoes a filamentation process analogous to a passive tracer in incompressible 2-D turbulence when the rate of strain variance exceeds relative vorticity variance:

$$S_s^2 + S_n^2 > \zeta^2 \, . \tag{3}$$

Equation (3) is simply the Okubo-Weiss criterion [e.g., Provenzale (1999)].

b. Potential Vorticity

The (quasigeostrophic) potential vorticity equation is [Müller (1976)]:

$$(\partial_t + \overline{u}\partial_x + \overline{v}\partial_y)(\partial_x^2 \Phi + \partial_y^2 \Phi + \partial_z [\frac{f^2}{N^2} \partial_z \Phi] + \beta y) =$$

$$\partial_x[\partial_x\overline{v''u''} + \partial_y\overline{v''v''} + \partial_z(\overline{v''w''} + \frac{f}{N^2}\overline{b''u''})]$$
$$-\partial_y[\partial_x\overline{u''u''} + \partial_y\overline{u''v''} + \partial_z(\overline{u''w''} - \frac{f}{N^2}\overline{b''v''})] + \mathcal{H} \tag{4}$$

in which $\mathcal{H}$ represents modification of the mean buoyancy profile through diabatic processes, Φ is the geostrophic streamfunction ($\Phi = \overline{\pi}/f$ with Coriolis parameter f) and pressure $\overline{\pi}$ is defined in the absence of the internal wavefield. For parcels that do not make excursions into the mixed layer, $\mathcal{H} = \partial_z \frac{f}{N^2}\partial_z(K_\rho \overline{b}_z)$. In the background wavefield $K_\rho \cong 5 \times 10^{-6}$ m^2 s^{-1}. The potential vorticity fluxes associated with this background diapycnal process acting on the mean buoyancy profile are an order of magnitude smaller than the observed mesoscale eddy potential vorticity flux divergence. Diabatic effects are thus excluded from consideration below and the issue will be revisited in the Discussion.

Assuming a scale separation and *local* plane wave solution, Müller (1976) demonstrates that the source terms in the potential vorticity equation can be cast as the horizontal curl of the pseudomomentum ($\mathbf{k}n$) flux divergence:

$$\partial_x[\partial_x\overline{v''u''} + \partial_y\overline{v''v''} + \partial_z(\overline{v''w''} + \frac{f}{N^2}\overline{b''u''})]$$
$$-\partial_y[\partial_x\overline{u''u''} + \partial_y\overline{u''v''} + \partial_z(\overline{u''w''} - \frac{f}{N^2}\overline{b''v''})] =$$
$$-\partial_x \nabla \cdot \int d^3k\; n(\mathbf{k},\mathbf{x},t)\; l\; \mathbf{C_g} + \partial_y \nabla \cdot \int d^3k\; n(\mathbf{k},\mathbf{x},t)\; k\; \mathbf{C_g} \tag{5}$$

with 3-D wave action spectrum $n \equiv E/\omega$, group velocity $\mathbf{C_g}$ and energy density $E = E_k + E_p$. The right-hand side of (5) directly states that an internal wave packet spatially localized in *both* horizontal dimensions carries with it a potential vorticity perturbation associated with the envelope structure of the wave packet, Bretherton (1969); Bühler and McIntyre (2005). A plane wave solution having constant amplitude in both horizontal directions has no pseudomomentum flux divergence and consequently no potential vorticity signature. A plane wave extending to infinity in one direction has a pseudomomentum flux divergence, but no curl of that divergence field. Statements to the effect that internal waves have no potential vorticity signature [e.g. Lien and Müller (1992); Polzin et al. (2003)] assume this infinite plane wave structure.

Finally, for steady conditions, small amplitude waves in a slowly varying background containing gradients in both (x, y) dimensions have a nondivergent action flux, $\int d\mathbf{k}\; \nabla \cdot \mathbf{C_g} n = 0$ rather than a nondivergent momentum flux. As the two variables differ by the wavevector and the wavevector evolves in response to the background flow field via (2), one has the result that potential vorticity can be traded between the fast manifold [the right-hand side of (4)] and the slow manifold [the left hand side of (4)]. This result is consistent with the material conservation of potential vorticity, Haynes and McIntyre (1987). At stake is a question of how internal wave processes contribute to a mixing of the coarse grained potential vorticity defined by the Reynolds average $\overline{\psi}$.

c. Potential Enstrophy

The eddy potential enstrophy budget is obtained by first decomposing the low frequency field into mean and mesoscale eddy components $\overline{\psi} = \overline{\overline{\psi}} + \psi'$ with $\overline{\overline{\psi}}$ given by an additional time average, $\overline{\overline{\psi}} = \tau^{-1} \int_0^\tau \overline{\psi}\; dt$, over many eddy time scales. In practice, the averaging time τ

is defined by the length of the observational record. Multiplying (4) by the quasigeostrophic perturbation potential vorticity q' and averaging returns:

$$\frac{1}{2}\frac{\overline{\overline{d}}}{dt}\,q'^2+\overline{\overline{\mathbf{u}'q'}}\cdot\nabla_h\overline{\overline{q}}=-\overline{\overline{q'\,[-\partial_x\nabla\cdot\int d^3k\;n(\mathbf{k},\mathbf{x},t)\;l\;\mathbf{C_g}+\partial_y\nabla\cdot\int d^3k\;n(\mathbf{k},\mathbf{x},t)\;k\;\mathbf{C_g}]}} \quad (6)$$

in which $\frac{\overline{d}}{dt}$ represents the material derivative following the geostrophic flow, ∇_h is the 2-D horizontal gradient operator and $\nabla_h\overline{\overline{q}}$ is the background potential vorticity gradient.

If closure of mesoscale eddy - internal wave coupling through flux gradient relations can be justified, in which $-2\overline{u''v''}=\nu_h(\overline{v}_x+\overline{u}_y)$, $-\overline{u''w''}=\nu_v\overline{u}_z$, $-\overline{u''u''}=\nu_h\overline{u}_x$, $-\overline{v''v''}=\nu_h\overline{v}_y$, $-\overline{u''b''}=K_h\overline{b}_x$, and $-\overline{v''b''}=K_h\overline{b}_y$, considerable simplification results. The right-hand-side of the enstrophy equation, using the thermal wind relation and integrating by parts, can be rewritten as:

$$\frac{1}{2}\frac{\overline{\overline{d}}}{dt}\,q'^2+\overline{\overline{\mathbf{u}'q'}}\cdot\nabla_h\overline{\overline{q}}=-\frac{1}{2}\nu_h[\overline{\overline{(\zeta_x^2+\zeta_y^2)}}+\frac{f_o^2}{\overline{\overline{b}}_z}\overline{\overline{\zeta_z^2}}]-[\nu_v+\frac{f^2}{N^2}K_h][\overline{\overline{\zeta_z^2}}+\frac{1}{\overline{\overline{b}}_z}\overline{\overline{(\overline{b}_{xz}^2+\overline{b}_{yz}^2)}}]\,. \quad (7)$$

3. The LDE Enstrophy Budget

We are now in a position to ask how the generation of internal wave pseudomomentum by eddy–wave coupling can be cast as a nonconservative term in the eddy enstrophy budget (6) and thereby be linked to potential vorticity dynamics. Brown et al. (1986) use the LDE array data [1] to estimate the eddy thickness [$\eta'=f_0(\rho'/\overline{\overline{\rho}}_z)_z$] and relative vorticity (ζ') fluxes:

$$\begin{aligned}\overline{\overline{\mathbf{u}'\eta'}}&=(-0.79\pm0.53,-1.45\pm0.71)\times10^{-7}\ \mathrm{m\,s^{-2}}\\ \overline{\overline{\mathbf{u}'\zeta'}}&=(-1.57\pm1.51,1.95\pm1.54)\times10^{-8}\ \mathrm{m\,s^{-2}}.\end{aligned} \quad (8)$$

A map of planetary vorticity on the potential density $\sigma_\theta=27.0$ surface in Robbins et al. (2000) implies $\nabla_h\overline{\overline{q}}\cong(0,\beta)=(0,2\times10^{-11}\ \mathrm{m^{-1}\,s^{-1}})$ at the level of the current meter data (the density surface is at approximately 700 m and the current meters are located at approximately 630 m for these potential vorticity flux estimates), so that

$$\overline{\overline{\mathbf{u}'q'}}\cdot\nabla_h\overline{\overline{q}}\cong-2.5\times10^{-18}\ \mathrm{s^{-3}}\,.$$

In order to maintain the observed planetary vorticity field in steady state, these fluxes are balanced by nonconservative mechanisms acting on the eddy field. These nonconservative terms will be evaluated assuming that the mesoscale eddy – internal wave coupling can be cast as a viscous process:

$$\text{r.h.s. of (6)}=-\frac{1}{2}\nu_h[\overline{\overline{(\zeta_x'^2+\zeta_y'^2)}}+\frac{f_o^2}{\overline{\overline{b}}_z}\overline{\overline{\zeta_z'^2}}]-[\nu_v+\frac{f_o^2}{N^2}K_h][\overline{\overline{\zeta_z'^2}}+\frac{1}{\overline{\overline{b}}_z}\overline{\overline{(b_{xz}'^2+b_{yz}'^2)}}]$$

$$\overline{\overline{(\zeta_x'^2+\zeta_y'^2)}}=6.7\times10^{-21}\ \mathrm{m^{-2}s^{-2}}$$

$$\frac{f_o^2}{\overline{\overline{b}}_z}\overline{\overline{\zeta_z'^2}}=2.5\times10^{-20}\ \mathrm{m^{-2}s^{-2}}$$

[1] The LDE array is discussed in detail in Bryden (1982) and Brown and Owens (1981). See Section 5 for commentary regarding the limitations of the array data for this work.

$$\overline{\overline{\zeta_z'^2}} = 8.4 \times 10^{-17}\ \mathrm{m^{-2}s^{-2}}$$
$$\frac{1}{\overline{\overline{b}}_z}\overline{\overline{(b_{xz}'^2 + b_{yz}'^2)}} = 1.9 \times 10^{-16}\ \mathrm{m^{-2}s^{-2}}$$

The relative vorticity's horizontal gradient variance $\overline{\overline{(\zeta_x'^2 + \zeta_y'^2)}}$ was estimated as twice the squared difference of the two possible vorticity estimates at 825 m, divided by the separation between the northeast-center-northwest and northwest-center-southwest triangle centers. The vertical vorticity gradient variance ($\overline{\overline{\zeta_z'^2}}$) was estimated from the one possible (northeast-center-northwest) triangle. The horizontal thickness gradient variance ($\overline{\overline{b_{xz}'^2 + b_{yz}'^2}}$) was estimated as $f^2(\overline{\overline{u_{zz}'^2 + v_{zz}'^2}})$ using data from the central mooring and current meters located at approximately 400, 600 and 800 m. These gradient variance terms were estimated by Fourier transforming the respective time series and then integrating to a spectral minimum at about 0.3 cpd. Following the previous discussion, the interior viscosity coefficients are taken to be ν_h = 50 m^2 s^{-1} and $\nu_v + \frac{f^2}{N^2}K_h = 2.5 \times 10^{-3}$ m^2 s^{-1}.

The grand total of potential enstrophy dissipation is:

$$\text{r.h.s. of (6)} = -1.6 \times 10^{-18}\ \mathrm{s^{-3}}$$

which is of appropriate order of magnitude to balance the estimated enstrophy production. Internal waves may therefore play a significant role in the momentum/enstrophy/vorticity balances of the Gulf Stream Recirculation.

There are significant issues about whether the potential enstrophy gradient variance is resolved and whether representing mesoscale eddy – internal wave coupling as a length scale independent viscosity provides an accurate estimate of the potential enstrophy dissipation rate. These issues will be entertained after considering theoretical models of the coupling process.

4. Models of Coupling

A complicating factor is that the momentum flux anomaly and associated vorticity perturbation induced by a wave packet in the linear analysis are reversible in the sense that the mean state is unchanged after it's passage. Müller (1976) provides the insight that, if the result of nonlinearity is to relax the wavefield back to an isotropic state, it is possible for the associated vorticity perturbation to become permanent: nonlinearity enables a *net* transfer of energy and vorticity between mesoscale eddies and internal waves. This insight is at the heart of the calculation presented below.

The evolution of the internal wavefield is governed by a radiation balance equation:

$$\mathcal{L}n = T_r + S_o - S_i \equiv S \tag{9}$$

in which $\mathcal{L}$ is the Liouville operator $\mathcal{L} = \partial_t + (\mathbf{C_g} + \overline{\mathbf{u}}) \cdot \nabla_\mathbf{x} + \mathbf{r} \cdot \nabla_\mathbf{k}$ with group velocity $\mathbf{C_g} = \nabla_\mathbf{k}\omega$ and refraction rate $\mathbf{r}$ given by the ray equations: $\mathbf{r} = d\mathbf{k}/dt = -\nabla_\mathbf{x}\sigma$ (2). The term T_r represents transfer of action by nonlinearity, S_o represents sources and S_i sinks of wave action (n). This description assumes the wave phase varies much more rapidly than the background velocity field and stratification profile. In the absence sources, sinks and nonlinearity, (9) states that the action flux is nondivergent:

$$\int d^3k\ \mathcal{L}n = \nabla \cdot \int d^3k\ (\mathbf{C_g} + \overline{\mathbf{u}})\ n(\mathbf{k}, \mathbf{x}, t)\ = 0.$$

Given the identification of the refraction rate $\mathbf{r}$ with the eikonal relation (2), which in turn has solutions given by the Okubo-Weiss relation (3) for asymmetric flow fields and wavefields dominated by Doppler shifting, it should be of little surprise that (9) can admit to a linear wave stress – mean strain relation.

a. Müller (1976)

1) OVERVIEW

The quasigeostrophic potential vorticity (4) and radiation balance equation (9) form a coupled system. Müller closes the system by invoking perturbation expansions associated with $\mathcal{L}$ and n:

$$(\mathcal{L}_0 + \delta\mathcal{L})[n^{(0)} + n^{(1)} + ...] = S[n^{(0)}] + \frac{\delta S}{\delta n}[n^{(1)} + n^{(2)} + ...] \ , \tag{10}$$

in which $\mathcal{L}_0 = \partial_t + \mathbf{C_g} \cdot \nabla_\mathbf{x} + \mathbf{r^{(0)}} \cdot \nabla_\mathbf{k}$, $\delta\mathcal{L}$ is the perturbation introduced by the mean flow and $\delta S/\delta n$ denotes the functional derivative. The zeroth order equation describes the generation, propagation, interaction, and dissipation processes that set up the background internal wavefield. The first-order equation describes perturbations induced by wave–mean interactions and the relaxation of those perturbations by nonlinearity. The formal solution for $n^{(1)}$ is:

$$n^{(1)} = -D^{-1}[\delta\mathcal{L}n^{(0)}] \tag{11}$$

in which D^{-1} is the functional inverse of $D = \mathcal{L}_0 - \delta S/\delta n$. The keys to recognizing the importance of nonlinearity are (a), if $S = 0$, the average perturbation is $\overline{n^{(1)}} = 0$, and (b) nonlinear transfers conserve energy (ωn) and pseudomomentum ($\mathbf{k}n$), not their spatial fluxes. Wave propagation in geostrophic background flows is based upon a nondivergent action flux. In conserving energy and pseudomomentum, nonlinearity serves as a nonconservative process relative to the issue of linear wave propagation.

Müller assumes the zeroth order state is independent of horizontal azimuth, and the effect of the first-order wave fluxes on the mean is estimated by substituting the first-order wavefield ($n^{(1)}$) into the mean source terms. These are formally written as:

$$\mathcal{F}^{(1)ij} = \int d^3k \ f^{ij} \ D^{-1}[k^\alpha \frac{\partial}{\partial k^m} n^{(0)} \frac{\partial}{\partial x^m} \overline{u}^\alpha] \tag{12}$$

$$\mathcal{M}^{(1)\beta} = \int d^3k \ m^\beta \ D^{-1}[k^\alpha \frac{\partial}{\partial k^m} n^{(0)} \frac{\partial}{\partial x^m} \overline{u}^\alpha] \ . \tag{13}$$

Expressions for f^{ij} and m^β are algebraic functions of frequency and wavenumber and are given in Müller (1976). The notation attempts to follow that of Müller (1976) and summation over indices m and α is implied. The usage of f, β and m in (12) and (13) should not be confused with the definitions herein.

Formal inversion of $\delta S/\delta n$ [(10) and (11)] is intractable if nonlinearity is assumed to be represented by resonant wave–wave interactions and a full-blown kinetic equation. Further progress is possible by interpreting $\delta S/\delta n$ as a relaxation time scale:

- $D^{-1}[\Psi] = \tau_R(\mathbf{k}) \ \Psi \ .$ (14)

By casting the first order balance as a spatially and temporally local process, i.e. assuming that

- $\tau_R(\mathbf{k})$ does not depend upon the past history of a wave packet,

and further assuming that

- $\tau_R(\mathbf{k}) \cong 200$ hours, independent of $\mathbf{k}$,

Müller is able to make analytic progress and establish quantitative estimates of the coupling coefficients in terms of correlations between momentum flux cospectra $[C(m,\omega) + iQ(m,\omega)]$, power spectra $[P(m,\omega)]$ and the mesoscale gradients (Müller 1976):

$$\begin{aligned}
C_{u''v''}(m,\omega) + iQ_{u''v''}(m,\omega) \quad &\text{and} \quad \overline{v}_x + \overline{u}_y \equiv S_s; \\
P_{u''u''}(m,\omega) - P_{v''v''}(m,\omega) \quad &\text{and} \quad \overline{u}_x - \overline{v}_y \equiv S_n; \\
[C_{u''w''}(m,\omega),\ C_{v''w''}(m,\omega)] \quad &\text{and} \quad [\overline{u}_z,\ \overline{v}_z];\ \text{and} \\
[C_{u''b''}(m,\omega),\ C_{v''b''}(m,\omega)] \quad &\text{and} \quad [\overline{b}_x,\ \overline{b}_y]\ .
\end{aligned} \tag{15}$$

A zero correlation is implied between

$$P_{u''u''}(m,\omega) + P_{v''v''}(m,\omega) \quad \text{and} \quad \overline{v}_x - \overline{u}_y \equiv\ \zeta\ .$$

The physical content of this result is contained within (3). Asymptotically, the rate of strain filaments a wave and the resulting momentum flux perturbation is uniquely related to the sign of the rate of strain. Relative vorticity simply rotates the horizontal wavevector. The resulting momentum flux perturbations can have either sign and hence the average kinetic energy–relative vorticity correlation is zero.

Integration over wavenumber and frequency returns a simple characterization of the coupling as a viscous process, for which: $-2\overline{u''v''} = \nu_h(\overline{v}_x + \overline{u}_y)$, $-\overline{u''w''} = \nu_v\overline{u}_z$, $-\overline{u''u''} = \nu_h\overline{u}_x$, $-\overline{v''v''} = \nu_h\overline{v}_y$, $-\overline{u''b''} = K_h\overline{b}_x$, and $-\overline{v''b''} = K_h\overline{b}_y$.

The disconcerting part of the story is that the quantitative predictions made by Müller are inconsistent with current meter observations obtained as part of the PolyMode program. In one case (Ruddick and Joyce 1979), the observed correlation between $\overline{u''w''}$ and vertical shear $\overline{u}_z$ was more than an order of magnitude smaller than the prediction. In another (Brown and Owens 1981), the observed correlation between $\overline{u''v''}$ and eddy gradients $\overline{v}_x + \overline{u}_y$ was more than an order of magnitude larger. See Section 1.d of the companion manuscript (Polzin 2009) for a summary of this segment of the observational literature.

2) Locality and Time Scales

My opinion is that the primary shortcoming of Müller (1976) is that it was written from the perspective that the thermocline was characterized by a diapycnal diffusivity of $K_\rho = 1 \times 10^{-4}$ m^2 s^{-1}, which implies a time scale of 5-10 days (200 hours) for nonlinear interactions to drain energy out of the background internal wavefield. Several decades of research (Polzin 2004a) has since demonstrated that the background wavefield is associated with a diffusivity of $K_\rho = 5 \times 10^{-6}$ m^2 s^{-1}, with corresponding time scale of 50-100 days. This is crucial for Müller's calculation. Müller's scheme invokes the ability of eddies to create anisotropic conditions out of an isotropic background wavefield. Nonlinearity is then invoked to relax the perturbed internal wavefield back to an isotropic state, and it is this relaxation that creates a permanent exchange of pseudomomentum for potential vorticity. With order of magnitude larger relaxation times, larger scale internal waves can propagate through an eddy-wave interaction event and on to another one in which the original wave-mean perturbation is erased, providing

minimal permanent exchange of pseudomomentum and vorticity. These propagation effects can be substantial.

Müller proposes that, *if* nonlocal effects were to be considered important, an order of magnitude estimate of the functional D^{-1} is provided by :

$$D^{-1} \cong D_{eff}^{-1} = \tau_R/[1 + (\tau_R/\tau_p)^2] \; . \tag{16}$$

The factor τ_p represents a propagation time scale:

$$\tau_p^{-1} = \Omega + \frac{C_g^{(0)x}}{L_x} + \frac{C_g^{(0)y}}{L_y} + \frac{C_g^{(0)z}}{H} \; , \tag{17}$$

in which $L^x, L^y, H \text{ and } \Omega^{-1}$ represent the spatial and temporal scales of the mesoscale eddy field. The direct implementation of (17) is not straight forward: it does not include the presence of vertical boundaries or buoyancy frequency turning points nor does it address possible complexities of the observed mesoscale field (Freeland and Gould 1976), i.e. the possible coupling of barotropic and baroclinic modes and westward (but not poleward/equatorward or vertical) phase propagation. Since the path to a realistic accounting is not clear at this juncture, possible resonance effects will be ignored (I will assume $\Omega = 0$) and the propagation time scale will be implemented in the horizontal and vertical coordinates separately.

Owens (1985) estimates a zero crossing of the transverse velocity correlation function of 100 km from the LDE current meter data. The longitudinal velocity correlation function falls off more slowly and thus the longitudinal length scale is not resolved. For the purpose of producing theoretical estimates of the coherence functions, the horizontal propagation time scale will be naively estimated with $50 \leq L \leq 200$ km. Wunsch (1997) finds that gradients of low frequency velocity are largely confined to the first several vertical modes, and thus a vertical scale (H) representative of the baroclinic mode-1 ($H = 700$ m) is assumed for the vertical propagation time scale.

Here a cascade representation of nonlinearity Polzin (2004a) will be used to define the relaxation time τ_R. This formulation is based upon an energy equation:

$$\frac{\partial E^{\pm}(m,\omega,\theta)}{\partial t} \pm \frac{\partial [\mathbf{C_g} E^{\pm}(m,\omega,\theta)]}{\partial \mathbf{x}} + \frac{\partial F^{\pm}(m,\omega,\theta)}{\partial m} = \frac{1}{2m}[F^{\mp}(m,\omega,\theta) - F^{\pm}(m,\omega,\theta)] \; . \tag{18}$$

Energy densities associated with opposing wavevectors $\mathbf{k}$ and $-\mathbf{k}$ are represented by E^+ and E^-; $F^{\pm}$ is the transfer of energy density to smaller vertical scales and superscripts denote the sign of the vertical wavenumber and azimuthal angle θ. The group velocity ($\mathbf{C_g}$) is assumed to be sign definite and the direction of propagation is given by a corresponding ($\pm$) prefactor. The right-hand side of (18) serves to conserve pseudomomentum: For internal waves, pseudomomentum is a signed quantity. A choice was made in this cascade representation (18) to conserve pseudomomentum by backscattering wave energy between two waves of similar, but oppositely signed wavevectors, at a rate in proportion to the spectral transport of energy to smaller scales. The backscattering is consistent with observations of increasing vertical isotropy at small vertical wavelengths.

I regard the cascade representation as a heuristic high wavenumber closure scheme rather than a representation of resonant interactions. As a heuristic description, frequency and azimuthal domain cascades are neglected. The frequency cascade is believed to be of secondary

importance [Polzin (2004a)] and observational records do not contain information from which an azimuthal cascade could be defined. If the azimuthal cascade sets a shorter timescale, it would be more appropriate here. However, it is difficult to see how either might exceed the time scale defined below based upon the vertical wavenumber transports.

The transfer $F^{\pm}$ is given by:

$$F^{\pm}(m,\omega,\theta) = a\, m^4\, N^{-1}\, \phi(\omega)\, E^{\pm}(m,\omega,\theta)\, E(m)\ , \tag{19}$$

with $a = 0.20$ and

$$\phi(\omega) = [(\omega^2 - f^2)/(N^2 - \omega^2)]^{1/2}\ .$$

The factor $E(m) = \int_f^N \int_0^{\pi} [E^+(m,\omega,\theta) + E^-(m,\omega,\theta)]\, d\omega d\theta$ is the energy spectrum integrated over frequency ω and horizontal azimuth θ. The functional representation denoted by ϕ implies increasing transport with increasing wave frequency, as suggested by the observations. The transport magnitude set by $a = 0.20$ is taken from the validation studies of Polzin et al. (1995) and Gregg (1989).[2]

I address the issue of defining the nonlinear time scale for specific moments of the momentum flux tensor by introducing a spatially homogeneous yet anisotropic perturbation $\Delta(m,\omega,\theta) = E^+ - E^-$. The governing radiation balance equation for Δ becomes:

$$\frac{\partial \Delta}{\partial t} + \frac{\partial}{\partial m} a m^4 N^{-1} \phi E(m) \Delta = -a m^3 N^{-1} \phi E(m) \Delta \tag{20}$$

Simply backscattering energy from $\mathbf{k}$ to $-\mathbf{k}$ does not alter the momentum flux: while $\mathbf{k}E/\omega$ and $-\mathbf{k}E/\omega$ have opposite signs, $\mathbf{C_g}(\mathbf{k}) = -\mathbf{C_g}(-\mathbf{k})$, and a momentum flux anomaly is not erased by backscattering. In order to define the time scale, one can either follow McComas and Müller (1981b)'s example of scaling the flux divergence as $\partial_m F \approx F/m$, or integrate (20) and the associated equation for $E^+ + E^-$ over frequency and horizontal azimuth and solve the coupled system of equations as in Polzin (2004b). Either procedure returns

$$\tau_R^{-1} = \frac{-1}{\Delta} \frac{\partial(\Delta)}{\partial t} = a m^3 N^{-1} \phi(\omega) E(m)\ . \tag{21}$$

Because of the non-specificity of the momentum flux anomaly associated with Δ, this cascade formulation permits identification of τ_R as a generic time scale for any specific moment of the momentum flux tensor.

3) The Horizontal Dimension

In the hydrostatic approximation, the horizontal viscosity becomes:

$$\nu_h = -\frac{1}{8} \int d^3k\, \frac{\omega^2 - f^2}{\omega^2}\, \frac{\omega\, k_h\, \tau_R}{1 + (\tau_R/\tau_p)^2} \frac{\partial n_3^{(0)}}{\partial k_h}\ , \tag{22}$$

in which k_h represents the magnitude of the horizontal wavevector components, $k_h = (k^2 + l^2)^{1/2}$

The zeroth order wavefield is represented using the Garrett and Munk (GM76) distribution,

$$E_2^{(0)}(m,\omega) = \frac{B}{(m_o^2 + m^2)} \frac{2f}{\pi} \frac{1}{\omega(\omega^2 - f^2)^{1/2}} \tag{23}$$

[2] there is a typo in (Polzin et al. 1995) that leads to a being misquoted as $a = 0.1$ in (Polzin 2004a).

with a slight modification. The spectral level is set by the dimensional constant B so that the total energy is 30×10^{-4} m^2 s^{-2} at $N_o = 3$ cph. A low-wavenumber roll-off m_o equivalent to mode-4 (not mode-3) is used to obtain both an appropriate total energy and high vertical wavenumber shear spectral density ($7N^2/2\pi$ s^{-2} rad m^{-1}). See the Appendix of Gregg and Kunze (1991) for details. The relation between the 2-D energy spectrum and a 3-D isotropic action spectrum dictates:

$$n_3^{(0)}(m,\omega) = E_2^{(0)}(m,\omega)/k_h\omega \ , \tag{24}$$

so that with $\tau_p = L/C_g^h$ (22) becomes:

$$\nu_h = \frac{fN^2}{4\pi a}\int_f^N \int_0^\infty \frac{[4\omega^2 - 3f^2]\ d\omega dm}{\omega^3 m^3 [\omega^2 + [\frac{N^3(m_o^2+m^2)}{Lam^4B}]^2]} \ . \tag{25}$$

Numerical evaluation returns

$$\nu_h \cong 50 \ \mathrm{m^2 s^{-1}} \tag{26}$$

for parameters (31^o latitude, N=2.6 cph, L=100 km) appropriate to the Polymode LDE data. The parameter regime is such that numerical evaluation also suggests an approximate linear dependence upon N, spectral amplitude B and eddy length scale L. The viscosity coefficient depends only weakly upon the strength of the cascade process (a) and the Coriolis parameter f. These dependencies come with a note of caution: *they may pertain only to the GM spectrum*. Müller's estimate was $\nu_h \cong 7$ m^2 s^{-1}, lower than that estimated here. That low estimate results from a relaxation time τ_R significantly smaller than implied by (21).

Direct comparison with the observed coherence functions presented in the companion paper (Polzin 2009) can be had be multiplying the integrand of (25) by the appropriate strain estimate [$\overline{|\ S_n\ |} = 1.41 \times 10^{-6}$ s^{-1} or $\overline{|\ S_s\ |} = 1.07 \times 10^{-6}$ s^{-1}] and dividing by the GM–$P_{uu}^{1/2}P_{vv}^{1/2}$ power spectral density functions. So constructed, the model coherence function estimates mimic the observed estimates (Fig. 1) reasonably well. Coherence function estimates tend to zero as ω approaches f and attain levels of 0.05–0.1 within the continuum frequency band. The observed cospectral estimates tend to increase towards higher frequency whereas the theoretical prediction decreases. Coherence function levels using $L = 100$ and $L = 200$ km tend to bracket the observations.

A second comparison can be made by comparing cumulative integrals of the observed coherence functions normalized by the respective rate of strain with their counterparts based upon (25), Fig. 2. In this instance semidiurnal frequencies make a significant contribution to the shear stress – rate of strain relation and so a second comparison is made by excluding semidiurnal frequencies from the cumulative integrals of the observed coherence functions. In so doing, the frequency integrated estimates of horizontal viscosity of 30-40 m^2 s^{-1} are bounded by the theoretical estimates with length scales of 50-100 km. Two details are worth noting. The first is that near-inertial frequencies make a larger contribution in the observations than in the theory. The observed background frequency spectrum from this region (Polzin et al. 2007) contains significantly more near-inertial than the GM model upon which the theoretical estimate is based. Second, the shear component of the rate of strain has its extensive axis oriented along in the NE-SW and NW-SE directions. This is essentially parallel to the crests and troughs of a topographic Rossby wave noted at the beginning of the LDE. It may be that the longer length scales in this direction enable a coupling between the topographic Rossby wave and a low-mode baroclinic tide emanating from the Blake Escarpment (Hendry 1977).

The agreement is impressive given the relatively unsophisticated treatment of the relaxation mechanism, the propagation time scale and unquestioned assumption that the GM spectrum is an adequate representation of the local background wavefield.

4) THE VERTICAL DIMENSION

In the hydrostatic approximation, the effective vertical viscosity becomes:

$$\nu_v + \frac{f^2}{N^2} K_h = \frac{1}{2} \int d^3k \, \frac{\omega^2 - f^2}{\omega^2} \, \frac{\omega \, k_h^2}{m} \frac{\tau_R}{1 + (\tau_R/\tau_p)^2} \frac{\partial n_3^{(0)}(k_h, m)}{\partial m} \, . \tag{27}$$

For a GM wavefield (23) and with $\tau_p = H/C_g^z$, this translates into:

$$\nu_v + \frac{f^2}{N^2} K_h = \frac{f}{\pi a} \int_f^N \int_0^\infty \frac{(\omega^2 - f^2)[2m_o^2\omega^2 - 3(m_o^2 + m^2)f^2]}{\omega^3 m^3 (m_o^2 + m^2)} \frac{d\omega dm}{[\omega^2 + [\frac{N^2(m_o^2+m^2)(\omega^2-f^2)^{1/2}}{Ham^4B}]^2]} \, . \tag{28}$$

Direct comparison with the observed coherence function estimate is possible by multiplying the integrand of (28) by the observed rms shear, $[(\overline{u}_z^2 + \overline{v}_z^2)/2]^{1/2} = 1.42 \times 10^{-4}$ s^{-1}. The resulting coherence estimates are near zero at high frequencies and negative at near-inertial, and qualitatively mimic the observations, Fig. (3). The resulting integral is distinctly negative, $\nu_v + \frac{f^2}{N^2} K_h = -8 \times 10^{-3}$ m^2 s^{-1}, rather than the observed positive value, $\nu_v + \frac{f^2}{N^2} K_h = 3 \times 10^{-3}$ m^2 s^{-1}. The difference between observed and predicted exchange coefficients is associated with small but distinctly positive coherence function estimates at high frequency, Fig. 3, and dominance of the $u''w''$ and $v''w''$ cospectra by high frequency contributions, Fig. 4.

The near zero values of the coherence function predictions using the GM76 spectrum are easily appreciated. In the high-frequency, high-vertical wavenumber limits, a power-law characterization of the 2-D energy spectrum and resulting 3-D action spectrum results in:

$$E_2(\omega, m) \propto \omega^{-s} m^{-t} \rightarrow n_3(\mathbf{k}) \propto (\frac{m}{k_h})^s (\frac{1}{m})^t \frac{1}{k_h^2} \, .$$

For the GM76 spectrum, $(s, t) = (2, 2)$ and $n_3(\mathbf{k}) \propto k_h^{-4} m^0$, and thus flux-gradient representations in the vertical wavenumber domain will predict minimal spectral transports (McComas and Bretherton 1977).

The observations and theoretical estimates of the vertical exchange coefficient are both much smaller than Müller's prediction of $\nu_v + \frac{f^2}{N^2} K_h \cong 0.45$ m^2 s^{-1}. Müller's large estimate is a product of neglecting propagation effects for buoyancy frequency waves of large vertical scales. That local treatment of (27) includes regions of the spectral domain ($m \cong m_o$) having $\partial_m n \neq 0$.

Caveats about the relatively unsophisticated treatment of the relaxation mechanism, uncertainties regarding the propagation time scale and the unquestioned assumption that the GM spectrum is an adequate representation of the local background wavefield again pertain.

b. Variants of the Müller (1976) model

1) RUDDICK AND JOYCE (1979)

Ruddick and Joyce (1979) note that Müller (1976)'s zeroth order wavefield is specified as the isotropic universal (GM) model in an Eulerian frequency coordinate. They argue that

the relaxation process could very well be toward an equilibrium spectrum with an intrinsic frequency coordinate. They find just such a solution to the radiation balance equation and note that it has a nondivergent momentum flux. Their interpretation is that this 'noninteracting state' provides much smaller deviations from equilibrium which, in turn, implies a much smaller viscosity.

My issue with Ruddick and Joyce (1979)'s comments is that their work concerns a greatly simplified vertical balance in which the mean velocity is considered to be a function only of the vertical coordinate: $[\overline{u}, \overline{v}] = [\overline{u}(z), 0]$. In this symmetric state, critical layers are approached as $\omega \to f$ and wave momentum is conserved (Andrews and McIntyre's generalized Eliassen-Palm flux theorem). The vertical wavenumber experiences linear growth with time and is independent of the evolution of the horizontal. In the three dimensional problem under consideration here, the critical layer is altered to a condition that the aspect ratio of the wave and mean flow be similar and wave momentum is not conserved. The vertical wavenumber evolves exponentially in time and is slaved to the horizontal. The behavior of the wave-mean interaction problem in three dimensions is different from that in one or two, Polzin (2008).

2) WATSON (1985)

The genesis of Watson (1985) is a recognition that there is no mechanism in the resonant interaction scheme of McComas and Müller (1981a) for transporting energy within the high vertical wavenumber ($100 \geq \lambda_v \geq 10$ m) near-inertial ($f < \omega \leq 2f$) frequency band toward even higher vertical wavenumber. The purpose of Watson (1985) was to formulate a radiation balance representation of wave–mean interactions in this band to transport action to a sink at $\lambda_v < 10$ m.

An ingredient of that representation is an estimate of the vertical and horizontal viscosity representing coupling of internal waves to mesoscale eddies. The coupling coefficient is estimated from kinetic theory as a variant of the induced diffusion mechanism: a near-inertial wave scatters from a (much) lower frequency and much larger scale mesoscale eddy field to transfer action to another near-inertial wave of nearly identical wavenumber.

A fundamental objection to this effort is phenomenological: Watson (1985)'s representation of wave–mean interactions assumes that the high wavenumber near–inertial waves execute a random walk associated with *many* individual scatterings. My perception is that such waves are subject to nonlinearity and will dissipate in a *single* event. In Polzin (2008) I document a $\lambda_v = 60$ m near–inertial wave interacting with mesoscale eddies. Estimates of a dissipation time scale through finescale parameterization schemes are 2-3 days for this wave, which is shorter than the $O(10)$ day time scale for advection to terminate the interaction event. Nonlinearity makes a significant contribution in this band even though there is no representation in the resonant interaction scheme for transferring this variance to smaller scales.

3) THE BOUNCE

As formulated, these models assume a constant buoyancy frequency. Waves are free to propagate in the vertical and will terminate an interaction event on a time scale $\tau_p = H/C_g^z$. Waves of sufficiently high frequency, however, will encounter turning points where their intrinsic frequency approaches that of the local stratification rate $N(z)$. Curiously, the negative vertical stress - vertical shear correlation occurs for waves that potentially encounter a buoyancy frequency turning point (Polzin 2009). The presence of turning points and a boundary can give

rise to a variant of the wave capture scenario.

In a deformation strain horizontal wavenumber magnitude asymptotically increases. Vertical wavenumber undergoes either an increase or decrease, but at both surface reflection or turning point there will be a sign change and opposing time evolution of the vertical wavenumber. Over many reflections and turning points, horizontal wavenumber magnitude increases, the vertical wavenumber remains nearly constant and consequently the intrinsic frequency increases. Such a wave will become progressively trapped in regions of higher and higher buoyancy frequency. A high frequency wave reported in Joyce and Stalcup (1984) may represent such an event. It is not clear that this phenomenology is appropriately represented in (16).

5. Array Resolution Issues

The LDE array was specifically designed to estimate terms in the quasigeostrophic potential vorticity equation with mooring spacing to optimally sample the deformation scale horizontal velocity gradients. One measure of the quality of the horizontal gradient estimates for a quasigeostrophic flow is given by Bryden (1976):

$$R = \frac{\overline{\overline{\mid \overline{u}_x + \overline{v}_y \mid}}}{\overline{\overline{\mid \overline{u}_x \mid}} + \overline{\overline{\mid \overline{v}_y \mid}}},$$

in which horizontal non-divergence implies $O(\zeta/f)$ values of R. Record length estimates of R are 0.3-0.5, (Brown and Owens 1981), an order of magnitude larger than the Rossby number. The large R values result in part from spatial aliasing as the horizontal divergence has significant contributions from spatial scales smaller than those that characterize the velocity. The lack of adequate spatial resolution implies the estimates of relative vorticity gradient variance and enstrophy dissipation are biased. In contrast, there is a tendency for the potential vorticity flux estimates to be coherent across the array (not shown here), implying that the flux is dominated by relatively large horizontal scales.

To assess the bias of the enstrophy dissipation estimate, I pursue the following consistency check. The estimates of kinetic energy, enstrophy, enstrophy gradient variance and enstrophy dissipation can be represented as the following moments of the kinetic energy spectrum:

variable	estimated	"fully resolved"	(29)
E_k	$\int_0^\infty E_k(k_h)\, dk_h$	$\int_0^{k_h^c} E_k(k_h)\, dk_h$	
$2\nu\zeta^2$	$2\int_0^\infty \nu_o k_h^2 sinc^2(\frac{k_h L_{fd}}{2\pi}) E_k(k_h)\, dk_h$	$2\int_0^{k_h^c} \nu(k_h) k_h^2 E_k(k_h)\, dk_h$	
ζ^2	$\int_0^\infty k_h^2 sinc^2(\frac{k_h L_{fd}}{2\pi}) E_k(k_h)\, dk_h$	$\int_0^{k_h^c} k_h^2 E_k(k_h)\, dk_h \propto \ln k_h^c$	
$\mid \nabla_h \zeta \mid^2$	$\int_0^\infty k_h^4 sinc^4(\frac{k_h L_{fd}}{2\pi}) E_k(k_h)\, dk_h$	$\int_0^{k_h^c} k_h^4 E_k(k_h)\, dk_h \propto (k_h^c)^2$	
$\frac{1}{2}\nu \mid \nabla_h \zeta \mid^2$	$\frac{1}{2}\int_0^\infty \nu_o k_h^4 sinc^4(\frac{k_h L_{fd}}{2\pi}) E_k(k_h)\, dk_h$	$\frac{1}{2}\int_0^{k_h^c} \nu(k_h) k_h^4 E_k(k_h)\, dk_h \propto k_h^c$	

Enstrophy and relative vorticity gradient variance estimates presented in Section 3 used a first difference scheme. The transfer function for a first difference operator over a length scale L_{fd} differs from the gradient by factor of $sinc(k_h L_{fd}/2\pi)$ in which $sinc(x) = sin(\pi x)/\pi x$. The

observed enstrophy gradient variance is approximately $(\zeta/L_{fd})^2$ rather than $(\zeta/L_d)^2$, which is consistent with the enstrophy gradient variance being dominated by scales smaller than L_d and raises concerns that those estimates are not resolved. To estimate the degree of bias, the first difference estimates can be compared to 'fully resolved' quantities determined by integrating the formulae to scales $1/k_h^c$ where the spectrum rolls off due to dissipation. The scale $1/k_h^c$ can be identified as the scale at which eddy potential vorticity is transfered to relative vorticity associated with the dipole structure of a wave packet. The finite difference estimates would be considered resolved in the two agree.

The estimates of energy and enstrophy dissipation are the product of the gradient variances and a coupling coefficient. From (25) one can anticipate the horizontal viscosity to be scale dependent, $\nu_h \propto k_h^{-1}$. The observed viscosity represents the coupling between the wave stress and resolved horizontal gradients, which are characterized by scales of approximately $L_d/2$. Thus as an *ad hoc* generalization:

$$\nu(k_h) = \frac{2\nu_o}{k_h L_d},$$

with $\nu_o = 50$ m^2 s^{-1} . Within the nominal enstrophy cascade regime, $E_k(k_h) \propto k_h^{-3}$, so that integrals representing enstrophy, relative vorticity gradient variance and enstrophy dissipation do not converge unless an explicit dissipation scale $1/k_h^c$ is invoked.

Particularly problematic is the attempt at estimating the enstrophy dissipation as the product of a significantly underestimated relative vorticity gradient variance with a horizontal viscosity (ν_o) unrepresentative of the scales which dominate that variance. To be quantitative I have taken the kinetic energy spectrum from AVISO[3] averaged over an extended area of the Western North Atlantic, extended the spectrum at wavenumbers greater than 3×10^{-5} m^{-1} with a k_h^{-3} power law, normalized the spectrum to the LDE array eddy kinetic energy estimate at 800 m and then integrated the spectral moments out to $2\pi/k_h^c = 10$ km. The factor of two agreement between the array estimates and the nominal finite difference moments, Table 1, lends credence to the methodology. My first difference estimate of enstrophy dissipation is almost an order of magnitude smaller than the "resolved" moment for a k_h^{-3} spectrum.

I conclude that the enstrophy dissipation estimate may be biased low. But then we are precisely where we started: an assertion that mesoscale eddy – internal wave coupling *may* result in enstrophy dissipation making an $O(1)$ contribution to the enstrophy variance equation.

Similar considerations apply to the vertical coordinate if viable theoretical estimates can be formulated and length scale variability identified.

6. Summary and Discussion

a. Summary

Current meter array data from the Local Dynamics Experiment (LDE) of the PolyMode field program were used in investigate the coupling of the mesoscale eddy and internal wave fields in the Southern Recirculation Gyre of the Gulf Stream. The coupling was characterized as a viscous process. In terms of momentum budgets, the transfer of eddy vorticity to internal wave pseudomomentum *may* play an $O(1)$ role in the eddy potential enstrophy budget. These results may be specific to the LDE region, which is situated at the exit of the Southern Recirculation Gyre. Further research is required to extrapolate these results.

[3]Spectrum supplied by Rob Scott, p.c. 2008.

A modified version of the mesoscale eddy–internal wave coupling mechanism described by Müller (1976) is used to predict an effective horizontal viscosity of 50–100 $m^2\ s^{-1}$. This result is in good agreement with observations obtained during the Local Dynamics Experiment ($\nu_h \cong 50\ m^2\ s^{-1}$). Similar modifications to Müller's theory for the coupling between vertical eddy gradients and vertical wave fluxes results in a prediction for an effective vertical viscosity of $-8 \times 10^{-3}\ m^2\ s^{-1}$ which is inconsistent with the observed value of $2.5 \times 10^{-3}\ m^2\ s^{-1}$. A possible reason for this discrepancy lies in the differences between the GM76 spectrum used to make the theoretical prediction and the observed spectrum.

Subtle differences between the regional background spectrum and the GM model are documented in Polzin et al. (2007). Most notably, the observed background spectrum is nonseparable in the frequency-vertical wavenumber domain with near-inertial waves being much more bandwidth limited than the internal wave continuum. High wavenumber/frequency power laws of the observed spectrum also differ from the GM model. It is difficult to further refine the theoretical estimates of eddy-wave coupling without having a 2-D vertical wavenumber–frequency spectrum on which to base the calculations.

This study comes with many caveats:

- First and foremost is that the LDE array does not spatially resolve the enstrophy gradient variance. However, the estimate of enstrophy dissipation appears to be biased low, and thus the claim that enstrophy dissipation *may* play an $O(1)$ role in the enstrophy budget is reinforced.

- The maximum observational record length for the LDE array data discussed in Section (3) is 15 months, but the failure of certain instruments reduces the usable record length to 225 days. Stable estimates of time mean quantities typically require averaging periods of order 500 days (Schmitz 1977). The mean quantities quoted here represent record length means with associated record length uncertainties. See Bryden (1982) and Brown et al. (1986) for further discussion of these uncertainties. I note, however, that the available 15 month estimates are consistent with the 225 day record means (to within uncertainty). Any differences do not change the interpretation presented here.

- The estimated viscosity coefficients could vary significantly in response to variability in the amplitude and spectral characteristics of the internal wavefield. In the scenario considered by Müller (1976), the net transfers of energy and momentum between eddies and waves is accomplished by nonlinearity relaxing wavefield perturbations back to an isotropic state. The strength of the nonlinearity will varying in response to variability in the background wavefield. Characterization of variability in response to spatial/temporal variations of sources and sinks is an open question.

- The characterization of enstrophy dissipation through a flux-gradient relation (15) necessarily omitted flux divergence terms and thus the flux-gradient characterization need not completely characterize the eddy-wave coupling process.

- The characterization of the coupling through a flux gradient relation applies only to quasi-geostrophic flows in which the flow field is horizontally nondivergent to O(Rossby number squared). Symmetric flow structures such as rings and jets are not coupled in the same manner.

The discussion below tries to flesh out some of the broader implications of eddy-wave coupling.

b. Discussion

1) THE END OF THE ENSTROPHY CASCADE

Potential vorticity is conserved in the absence of diabatic processes and friction. The dominant intellectual prejudice in Physical Oceanography is to regard frictional processes as being turbulent (essentially diabatic) in nature and sufficiently weak within the oceanic interior that potential vorticity modification following a parcel occurs only at the boundaries.

Diabatic mixing occurs in the ocean when small-scale shears become strong enough to overturn the stable stratification. Geostrophically balanced eddies are not efficient at generating small-scale shear as enstrophy conservation arrests the transfer of energy to small scales. At small scales the mesoscale eddy kinetic energy spectrum scales with a power law of $E_k(k_h) \propto k_h^{-3}$. Thus the shear variance is independent of scale and typically so small that small-scale overturns (e.g., Kelvin-Helmhotz billows) do not develop. The picture is one of potential vorticity anomalies in the enstrophy cascade being filamented, collapsing, and eventually removed by ambient diabatic processes.

If, on the other hand, mesoscale eddies are coupled to the internal wavefield as described here, then the enstrophy cascade can be short-circuited. The exchange of eddy relative vorticity for wave pseudomomentum accomplishes enstrophy dissipation. The removal of energy into the internal wavefield implies a diabatic dissipation mechanism (ultimately through internal wavebreaking) even though the direct eddy–wave interaction is adiabatic.

One relevant question is, "at what scale does mesoscale eddy - internal wave coupling compete with nonlinearity on the slow manifold?" This is difficult to address with the data at hand, but consider an example (Wilson and Williams 2004) of an idealized eddy resolving model that has been used to explore eddy dynamics and the consequences eddies have for the mean circulation. A tentative generalization of such model behavior is that eddy fluxes typically are along, rather than across, mean potential vorticity contours, and that the mean tends to a state of potential vorticity homogenization, in which the down gradient potential vorticity flux contribution to the enstrophy budget is small. Wilson and Williams (2004) attribute this behavior to the eddy advection of enstrophy. The dominant balance in their enstrophy equation is between eddy advection (nonlinearity), $\overline{\overline{\mathbf{u}' \cdot \nabla q'^2}}$, and enstrophy production $\overline{\overline{\mathbf{u}' q'}} \cdot \nabla \overline{\overline{q}}$. The model used in Wilson and Williams (2004) employs a biharmonic mixing of momentum. This functional representation permits the creation of high enstrophy at the deformation scale and its dissipation at the smallest scales: large enstrophy gradients are permitted and eddy advection of these gradients balance the down gradient potential vorticity fluxes. Eddy enstrophy can then be carried to the boundary where it is efficiently dissipated. The biharmonic frictional coefficient $A_h = 2.5 \times 10^9$ m^4 s^{-1} used by Wilson and Williams (2004) implies a deformation scale ($L_d = 5 \times 10^4$ m) Reynolds number of:

$$u' L_D^3 / A_h \cong 2500$$

with rms velocity $u' = 0.05$ m s^{-1}. Given a viscous representation to the eddy-wave coupling mechanism, a deformation scale ($L_d = 5 \times 10^4$ m) Reynolds number is:

$$u' L_D / \nu_h \cong 50$$

with $\nu_h = 50$ m^2 s^{-1}. If variation of ν_h as $\nu_h \propto L$ is considered, the Reynolds number decreases with decreasing length scale, $Re \propto L$ in the enstrophy cascade regime. Based upon experience

with 3-dimensional turbulence, I suspect that this parameter regime may not exhibit an extended inertial subrange.

A second way of stating this is to consider the ratio between an enstrophy dissipation time scale $\tau_d = k_h^2 E_k / \frac{1}{2}\nu k_h^4 E_k$ and nonlinear time scale $\tau_{nl} 2/\Gamma$, with $\Gamma = (S_n^2 + S_s^2 - \zeta^2)^{1/2}$ an effective deformation scale strain rate. Unity values of this time scale ratio occur at horizontal wavelengths $\lambda_h = 10$ km.

Defining the end of the enstrophy cascade will be complicated as potential vorticity perturbations associated with the enstrophy cascade coexist with vortical modes (Polzin et al. 2003; Polzin and Ferrari 2004) and internal wave dipoles (Polzin 2008) on submesoscales.

2) Implications for the Slow Manifold – Fast Manifold Debate

The slow manifold – fast manifold moniker is a recognition that the equations of motion support two distinct linearized modes: fast gravity waves and slow motions in approximate geostrophic balance. The debate is essentially a question of whether initially balanced (geostrophically balanced) states can evolve without significant coupling to gravity waves.

With respect to mechanisms, the debate is cast either in terms of an analogy to to the forcing of linear acoustic waves by turbulence (vortical motions), e.g. Ford et al. (2000), or the linear instability of a parallel shear flow (notably a symmetric state), Molemaker et al. (2005). There is a growing body of evidence that such spontaneous forcing of the fast manifold is weak.

The thesis of this work is that internal waves can interact with geostrophically balanced flows, exchanging pseudomomentum, energy and potential vorticity without the requirement of diabatic effects or resonance conditions. In this study, asymmetry of the background and nonlinearity in the internal wavefield are the key properties associated with irreversible exchanges. Small amplitude waves propagating in a larger scale geostrophic flow field obey an action conservation principle. Since the horizontal wavevector evolves following a wave-packet in nonaxisymmetric background flows, it follows from (4) and (5) that a momentum flux divergence will induce a potential vorticity perturbation, and that this can be accomplished adiabatically. This vorticity perturbation is reversible in the sense that the mean state is unchanged after the passage of a linear packet. Müller (1976) provides the insight that, if the action of nonlinearity is to relax the wavefield back to an isotropic state, it is possible for the associated vorticity perturbation to become permanent: nonlinearity enables a *net* transfer of energy and vorticity between mesoscale eddies and internal waves.

An action conservation principle is essentially conservation of a real valued phase function [(2), see Andrews and McIntyre (1978)] and needs to be distinguished from an instability problem, which describes the transfer from slow to fast manifolds with a complex valued phase function. One can think of mesoscale eddy–internal wave coupling as an amplifier of a preexisting or externally forced finite amplitude wavefield rather than the spontaneous imbalance of a linear field. The issue of nonlinearity needs to be kept in mind when interpreting numerical simulations, such as those presented in Dritschel and Viùdez (2007). A nondimensional landmark is the ratio of linear to nonlinear timescale (17) in (16).

3) General Circulation Issues

At the LDE site we have an observation of potential vorticity fluxes. As the observed flux is directed across isopleths of background vorticity, that potential vorticity flux also represents potential enstrophy production. In steady state, either an advective flux divergence (nonlinear-

ity) or dissipation is required. I infer an approximate production–dissipation balance associated with mesoscale eddy – internal wave coupling.

This work started by noting the degree to which the symmetrically constrained Eliassen–Palm flux theorem (1) has focussed intellectual effort on understanding the effects of nonlinearity. I make the case in this manuscript that "dissipation" needs equal footing.

In a one-dimensional vertical advection - vertical diffusion balance of the buoyancy equation, diapycnal diffusivities of $O(1\times10^{-4}$ m^2 s$^{-1})$ are required to balance the upwelling of some 30×10^6 m^3 s^{-1} Bottom and Deep Waters produced in polar regions, Munk (1966). There may be sufficient diapycnal mixing above topographically rough regions driven by internal wave breaking (Polzin et al. 1997) or associated with topographically constrained passages (Polzin et al. 1996; St.Laurent and Thurnherr 2007) to upwell Deep and Bottom waters to Intermediate Water levels (1000-2000 m water depth over much of the World's Oceans). However, diapycnal mixing is sufficiently weak, $O(1 \times 10^{-5}$ m^2 s$^{-1})$, over much of the thermocline region [e.g. Ledwell et al. (1993)], that advocacy of a diapycnal advection-diffusion balance is difficult to defend.

Something must give, and the conceptual paradigm that supplants the vertical advection – vertical diffusion balance is that of Luyten et al. (1983), in which mean streamlines coincide with mean potential vorticity contours, with streamlines consisting of Rossby wave trajectories. A competing hypothesis is that, if one takes the ideal fluid limit of an adiabatic and inviscid interior and considers the effect of mesoscale eddies, mesocale variability will tend to produce interiors with small mean potential vorticity gradients, Rhines and Young (1982).

The relative contributions of eddies and interior diabatic processes to the mean potential vorticity balance of gyre interiors can be gauged by scale estimates of the respective terms: eddy contributions[4] are $\nabla \cdot \overline{q'\mathbf{u}'} \sim O(1 \times 10^{-7}\mathrm{m\,s^{-2}}/5 \times 10^6\mathrm{m})$ and diabatic effects[5] are $\partial_z f N^{-2} \partial_z K_\rho N^{-2} \sim O(10^{-4}\mathrm{s^{-1}} \times 10^{-5}\mathrm{m^2 s^{-1}}/(700\mathrm{m})^2$, an order of magnitude smaller.

My preference is to consider the upper limb of the Meridional Overturning Circulation to be closed along isopycnals with mesoscale eddy – internal wave coupling playing a significant role in potential vorticity modification. I emphasize the issue of potential vorticity modification as I put more weight on McCartney (1982)'s characterization of potential vorticity increase and water mass modification of Mode Waters along likely advection paths than the corresponding analyses of McDowell et al. (1982) and Keffer (1985).

4) Issues of Variability

Variability of the viscosity coefficients acting on the mesoscale field will depend upon variability in the background wavefield. Such variability exists [Polzin et al. (2007)]. A possible implication of this work is that the variability in both the mesoscale eddy field (Zang and Wunsch 2001) and the internal wavefield (Polzin et al. 2007) are related through mesoscale eddy–internal wave coupling. In terms of understanding the geographic variability of viscosity coefficients, there is a simplicity if the energetics of the internal wave field are dominated by an interior coupling to the mesoscale eddy field, as appears to be the case in the Southern Recirculation Gyre. This represents the dynamic balance advocated by Müller and Olbers (1975), albeit at somewhat reduced interaction rates. Simplicity is also attained if the mesoscale eddy

[4]Here I have taken the observed potential vorticity fluxes at the LDE site and divided by a length scale of 5000 km.

[5]Here I take f to be representative of 45° degrees latitude, a background diapycnal diffusivity of 1×10^{-5} m^2 s^{-1} and thermocline scale of 700 m.

spectrum rolls-off uniformly at the deformation radius and the propagation scales L_i in (17) can be related to L_d.

The internal wave–eddy coupling becomes more complicated if the geostrophic flow field locally forces the zeroth order wavefield though quasi-stationary internal lee wave generation. An associated issue is posed by non-equilibrium (vertically decaying) internal wave states associated with tidal forcing at mid-ocean ridges [Polzin (2004b)]. These factors may help explain why the mesoscale eddy field above the Mid-Atlantic Ridge tends to be more baroclinic than topologically smooth regions, Wunsch (1997).

I leave the reader with the following questions:

- How spatially variable are these effective viscosities? Are results from the Gulf Stream Recirculation applicable to more climatologically sensitive regions such as the Southern Ocean [(Naveira-Garaboto et al. 2004), (Polzin and Firing 1998)] or the Greenland–Iceland–Norwegian Seas, Naveira-Garaboto et al. (2005)?

- The behavior of simplified oceanic general circulation models depends upon how viscous damping is implemented [(Cessi and Ierley 1995), (Fox-Kemper and Pedlosky 2004)]. What happens to the behavior of the general circulation as the thermocline tightens, the eddy scale decreases, or the rms eddy velocity increases?

- One perspective of climate change is that temporal trends at increasingly longer time scales represent increasingly smaller imbalances in the equations of motion. If true, can we really claim to understand how the climate system works if GCMs are simply tuned to today's conditions and do not address the proper sub-grid scale physics?

Acknowledgments.

Much of the intellectual content of this paper evolved out of discussions with R. Ferrari. The manuscript benefitted from discussions with Brian Arbic, Rob Scott and a review provided by Peter Rhines. Salary support for this analysis was provided by Woods Hole Oceanographic Institution bridge support funds.

References

Andrews, D. G., J. R. Holton, and C. B. Leovy, 1987: *Middle Atmosphere Dynamics*. Academic Press, Orlando, 1–489 pp.

Andrews, D. G. and M. E. McIntyre, 1978: On wave action and its relatives. *J. Fluid. Mech.*, **89 (4)**, 647–664.

Bretherton, F. P., 1969: On the mean motion induced by internal gravity waves. *J. Fluid. Mech.*, **36**, 785–803.

Brown, E. D. and W. B. Owens, 1981: Observations of the horizontal interactions between the internal wave field and the mesoscale flow. *J. Phys. Oceanogr.*, **11**, 1474–1480.

Brown, E. D., W. B. Owens, and H. L. Bryden, 1986: Eddy-potential vorticity fluxes in the Gulf Stream Recirculation. *J. Phys. Oceanogr.*, **16**, 523–1531.

Bryden, H. L., 1976: Horizontal advection of temperature for low–frequency motions. *Deep-Sea Res.*, **23**, 1165–1174.

———, 1982: Sources of eddy energy in the Gulf Stream Recirculation Region. *J. Mar. Res.*, **40**, 1047–1068.

Bühler, O. and M. E. McIntyre, 2005: Wave capture and wave-vortex duality. *J. Fluid. Mech.*, **534**, 67–95.

Cessi, P. and G. R. Ierley, 1995: Symmetry-breaking multiple equilibria in quasigeostrophic, wind driven flows. *J. Phys. Oceanogr.*, **25**, 1996–1205.

Dritschel, D. G. and A. Viùdez, 2007: The persistence of balance in geophysical flows. *J. Fluid. Mech.*, **570**, 365–383.

Ertel, H., 1942: Ein neuer hydrodynamischer Wirbelsatz. *Meteorol. Z.*, **59**, 277–281.

Ford, R., M. E. McIntyre, and W. A. Norton, 2000: Balance and the slow quasimanifold: Some explicit results. *J. Atmos. Sci.*, **57**, 1236–1254.

Fox-Kemper, B. and J. Pedlosky, 2004: Wind-driven barotropic gyre I: Circulation control by eddy vorticity fluxes to an enhanced removal region. *J. Mar. Res.*, **62 (2)**, 169–193.

Freeland, H. J. and W. J. Gould, 1976: Objective analysis of mesoscale ocean circulation features. *Deep Sea Res.*, **23**, 915–923.

Gregg, M. C., 1989: Scaling turbulent dissipation in the thermocline. *J. Geophys. Res.*, **94**, 9686–9698.

Gregg, M. C. and E. Kunze, 1991: Shear and strain in Santa Monica Basin. *J. Geophys. Res.*, **96**, 16 709–16 719.

Haynes, P. H. and M. E. McIntyre, 1987: On the evolution of vorticity and potential vorticity in the presence of diabatic heating and frition or other forces. *J. Atmos. Sci.*, **44**, 828–841.

Hendry, R. M., 1977: Observations of the semidiurnal internal tide in the western north atlantic ocean. Philosophical Transactions of the Royal Society of London A, **286**, 1–24.

Hogg, N. G., 1983: A note on the deep circulation of the western North Atlantic: Its nature and causes. *Deep-Sea Res. I*, **30**, 945–961.

Jayne, S. R., N. G. Hogg, and P. Malanotte-Rizzoli, 1996: Recirculation gyres forced by a beta-plane jet. *J. Phys. Oceanogr.*, **24**, 492–504.

Johns, W. E., T. J. Shay, J. M. Bane, and D. R. Watts, 1995: Gulf Stream structure, transport, and recirculation near 68°W. *J. Geophys. Res.*, **100**, 817–838.

Joyce, T. M. and M. C. Stalcup, 1984: An upper ocean current jet and internal waves in a Gulf Stream Warm Core Ring. *J. Geophys. Res.*, **89**, 1997–2003.

Keffer, T., 1985: The ventilation of the World's Ocean: Maps of the potential vorticity fields. *J. Phys. Oceanogr.*, **15**, 509–523.

Ledwell, J. R., A. J. Watson, and C. S. Law, 1993: Evidence for slow mixing across the pycnocline from an open-ocean tracer-release experiment. *Nature*, **364**, 701–703.

Lien, R. and P. Müller, 1992: Consistency relations for gravity and vortical modes in the ocean. *Deep-Sea Res.*, **39**, 1595–1612.

Luyten, J. R., J. Pedlosky, and H. Stommel, 1983: The ventilated thermocline. *J. Phys. Oceanogr.*, **13**, 292–309.

McCartney, M. S., 1982: The subtropical recirculation of Mode Waters. *J. Mar. Res.*, **40 (suppl.)**, 427–464.

McComas, C. H. and F. P. Bretherton, 1977: Resonant interaction of oceanic internal waves. *J. Geophys. Res.*, **83**, 1397–1412.

McComas, C. H. and P. Müller, 1981a: The dynamic balance of internal waves. *J. Phys. Oceanogr.*, **11**, 970–986.

———, 1981b: Timescales of resonant interactions among oceanic internal waves. *J. Phys. Oceanogr.*, **11**, 139–147.

McDowell, S., P. Rhines, and T. Keffer, 1982: North atlantic potential vorticity and its relation to the general circulation. *J. Phys. Oceanogr.*, **12**, 1417–1436.

Molemaker, M. J., J. C. McWilliams, and I. Yavneh, 2005: Baroclinic instability and loss of balance. *J. Phys. Oceanogr.*, **35**, 1505–1517.

Müller, P., 1976: On the diffusion of momentum and mass by internal gravity waves. *J. Fluid. Mech.*, **77**, 789–823.

Müller, P. and D. J. Olbers, 1975: On the dynamics of internal waves in the deep ocean. *J. Geophys. Res.*, **80**, 3848–3860.

Munk, W., 1950: On the wind-driven circulation. *J. Meteor.*, **7**, 79–93.

———, 1966: Abyssal recipes. *Deep-Sea Res.*, **13**, 207–230.

Naveira-Garaboto, A., K. I. C. Oliver, A. J. Watson, and M.-J. Messias, 2005: Turbulent diapycnal mixing in the nordic seas. *J. Geophys. Res.*, **?**, xx–yy.

Naveira-Garaboto, A., K. L. Polzin, B. A. King, K. J. Heywood, and M. Visbeck, 2004: Widespread intense mixing in the deep Southern Ocean. *Science*, **303**, 210–213.

Owens, W. B., 1985: A statistical description of the vertical and horizontal structure of eddy variability on the edge of the Gulf Stream Recirculation. *J. Phys. Oceanogr.*, **15**, 195–205.

Polzin, K. L., 2004a: A heuristic description of internal wave dynamics. *J. Phys. Oceanogr.*, **34**, 214–230.

———, 2004b: Idealized solutions for the energy balance of the finescale internal wavefield. *J. Phys. Oceanogr.*, **34**, 231–246.

———, 2008: Mesoscale eddy - internal wave coupling. i. Symmetry, wave capture and results from the Mid-Ocean Dynamics Experiment. *J. Phys. Oceanogr.*, **?**, ?

———, 2009: Mesoscale eddy - internal wave coupling. ii. energetics and results from polymode. *submitted to J. Phys. Oceanogr.*, **?**, ?

Polzin, K. L., J. M. T. abd J. R. Ledwell, and R. W. Schmitt, 1997: Spatial variability of turbulent mixing in the abyssal ocean. *Science*, **276**, 93–96.

Polzin, K. L. and R. Ferrari, 2004: Isopycnal dispersion in natre. *J. Phys. Oceanogr.*, **34**, 247–257.

Polzin, K. L. and E. Firing, 1998: Estimates of diapycnal mixing using ladcp and ctd data from i8s. *International WOCE Newsletter*, **29**, 39–42.

Polzin, K. L., E. Kunze, J. M. Toole, and R. W. Schmitt, 2003: The partition of fine-scale energy into internal waves and subinertial motions. *J. Phys. Oceanogr.*, **33**, 234–248.

Polzin, K. L., Y. Lvov, and E. Tabak, 2007: The oceanic internal wavefield. I. Toward regional characterizations. *manuscript in preparation*.

Polzin, K. L., K. G. Speer, J. M. Toole, and R. W. Schmitt, 1996: Intense mixing of Antarctic Bottom Water in the equatorial Atlantic Ocean. *Nature*, **380**, 54–57.

Polzin, K. L., J. M. Toole, and R. W. Schmitt, 1995: Finescale parameterizations of turbulent dissipation. *J. Phys. Oceanogr.*, **25**, 306–328.

Provenzale, A., 1999: Transport by coherent barotropic vortices. *Ann. Rev. Fluid Mech.*, **31**, 55–93.

Rhines, P. B., 1979: Geostrophic Turbulence. *Ann. Rev. Fluid Mech.*, **11**, 401–441.

Rhines, P. B. and R. Schopp, 1991: The wind driven circulation: Quasi-geostrophic simulations and theory for nonsymmetric winds. *J. Phys. Oceanogr.*, **21**, 1438–1469.

Rhines, P. B. and W. R. Young, 1982: A theory of the wind driven circulattion. i. Mid-ocean gyres. *J. Mar. Res.*, **40 (suppl.)**, 559–596.

Robbins, P. E., J. F. Price, W. B. Owens, and W. J. Jenkins, 2000: The importance of lateral diffusion for the ventilation of the lower thermocline in the Subtropical North Atlantic. *J. Phys. Oceanogr.*, **67**, 67–89.

Ruddick, B. R. and T. M. Joyce, 1979: Observations of interaction between the internal wave-field and low-frequency flows in the north atlantic. *J. Phys. Oceanogr.*, **9**, 498–517.

Salmon, R., 1998: *Lectures in Geophysical Fluid Dynamics*. Oxford University Press, New York, 1–378 pp.

Schmitz, W. J., 1977: On the deep general circulation in the western North Atlantic. *J. Mar. Res.*, **35**, 21–28.

Schmitz, W. J., J. D. Thompson, and J. R. Luyten, 1992: The Sverdrup circulation for the Atlantic along 24°. *J. Geophys. Res.*, **97**, 7251–7256.

St.Laurent, L. C. and A. M. Thurnherr, 2007: Intense mixing of lower thermocline water on the crest of the Mid–Atlantic Ridge. *Nature*, **448**, 680–683.

Stommel, H., 1948: The westward intensification of wind-driven ocean currents. *Trans. Amer. Geophys. Union* , **29**, 202–206.

Watson, K. M., 1985: Interaction between internal waves and mesoscale flow. *J. Phys. Oceanogr.*, **15**, 1296–1311.

Wilson, C. and R. G. Williams, 2004: Why are eddy fluxes of potential vorticity so difficult to parameterize? *J. Phys. Oceanogr.*, **34**, 142–155.

Wunsch, C., 1997: The vertical partition of oceanic horizontal kinetic energy. *J. Phys. Oceanogr.*, **27**, 1770–1794.

Zang, X. and C. Wunsch, 2001: Spectral description of low-frequency oceanic variability. *J. Phys. Oceanogr.*, **31**, 3073–3095.

List of Figures

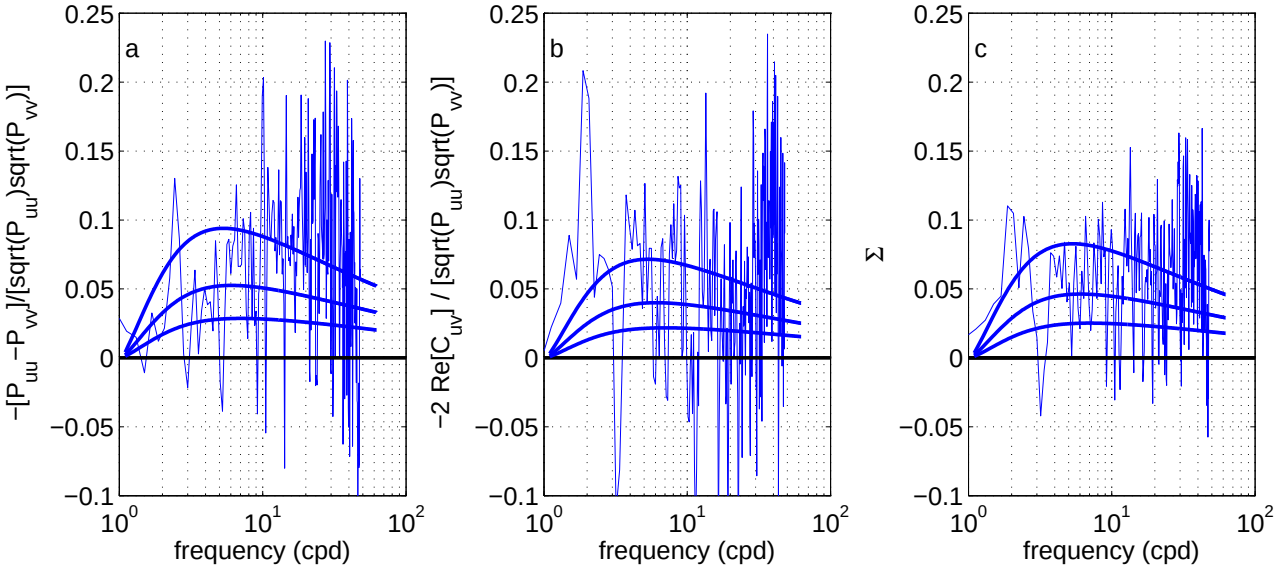

FIG. 1. Coherence functions created by averaging (a) $-sgn(S_n)[P_{u''u''} - P_{v''v''}]/P^{1/2}_{u''u''}P^{1/2}_{v''v''}$, (b) $-sgn(S_s)C_{u''v''}/P^{1/2}_{u''u''}P^{1/2}_{v''v''}$ with $C_{u''v''}$ being the real part of the $u''v''$ cross-spectrum and (c) the average of the preceding panels. Over plotted as thick lines are GM76 based estimates for the coherence functions using (25). These model coherence functions use eddy decorrelation scales of 50, 100 and 200 km, with model coherence increasing with increasing horizontal length scale L. Estimates are based upon 512 point transform intervals and averaging data from both triangles at 825 m water depth.

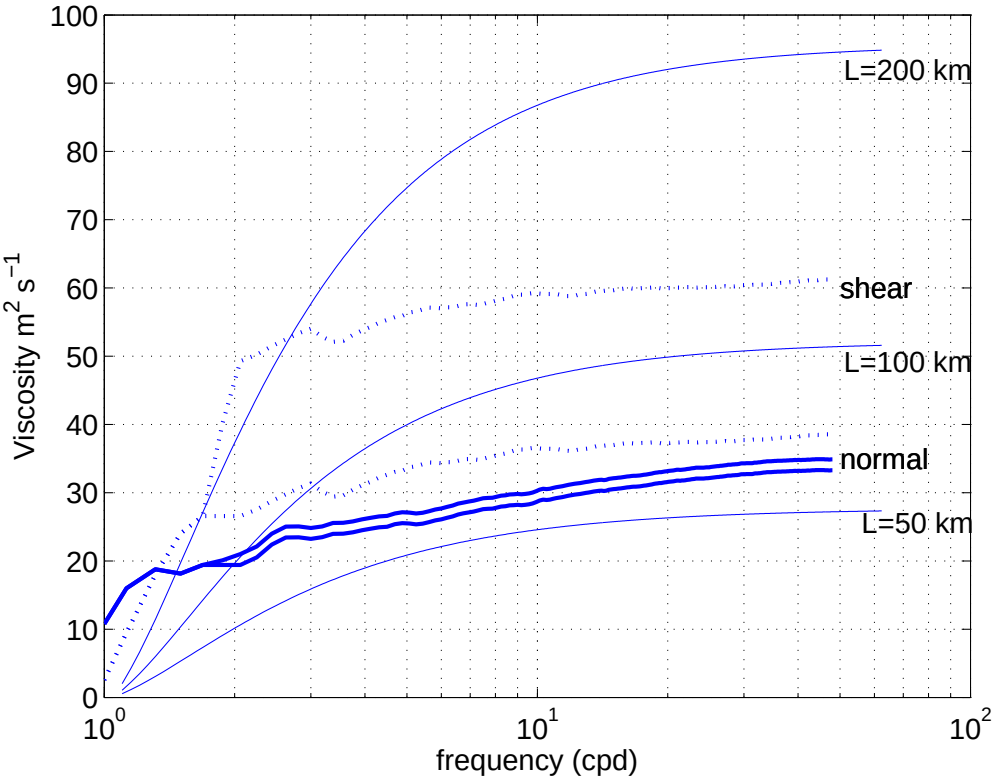

FIG. 2. Cumulative integrals of the spectral functions $-sgn(S_n)[P_{u''u''}-P_{v''v''}]$ (thick lines) and $-2sgn(S_s)C_{u''v''}$ (dashed lines), divided by rate of strain $\overline{\overline{\mid S_n \mid}}$ and $\overline{\overline{\mid S_s \mid}}$, to provide estimates of the horizontal viscosity ν_h. Two estimates of each appear. The lower curves ignore contributions at semi-diurnal frequencies. Over plotted as thin lines are GM76 based estimates for the corresponding viscosity estimate using (25). These estimates employ an eddy decorrelation scale of $L = 50$, 100 and 200 km.

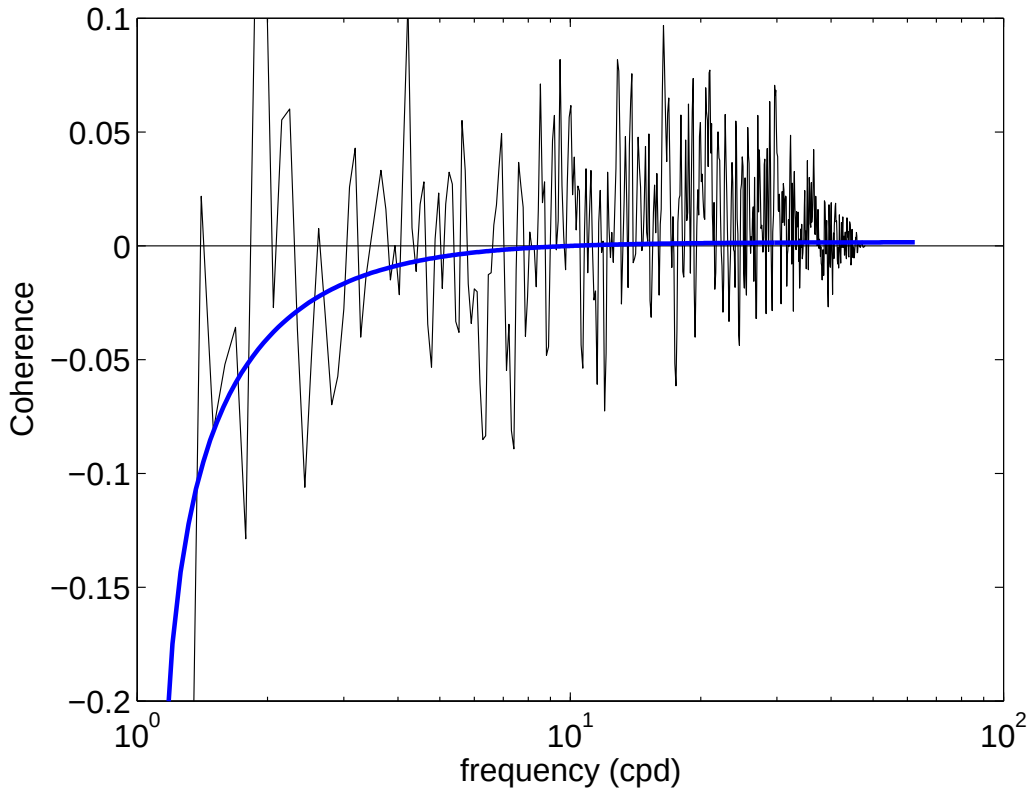

FIG. 3. Coherence function created by averaging $-sgn(\overline{u}_z)[C_{u''w''} - fN^{-2}C_{v''b''}]/T(\omega)P^{1/2}_{u''u''}P^{1/2}_{w''w''}$ and $-sgn(\overline{v}_z)[C_{v''w''} + fN^{-2}C_{u''b''}]/T(\omega)P^{1/2}_{v''v''}P^{1/2}_{w''w''}$. The factor $C_{x''y''}$ represents the real part of the $x''y''$ cross-spectrum. The transfer function $T(\omega) = (\omega^2 - f^2)/(\omega^2 + f^2)$ accounts for cancelation of the Reynolds stress by the buoyancy flux and renders the denominator consistent with the numerator. Over plotted as thick a line is a GM76 based estimate for the coherence functions using (28). The coherence estimates are based upon 1024 point transform intervals of data at both 600 and 825 m levels. Data are from the Center, Northeast and Northwest moorings.

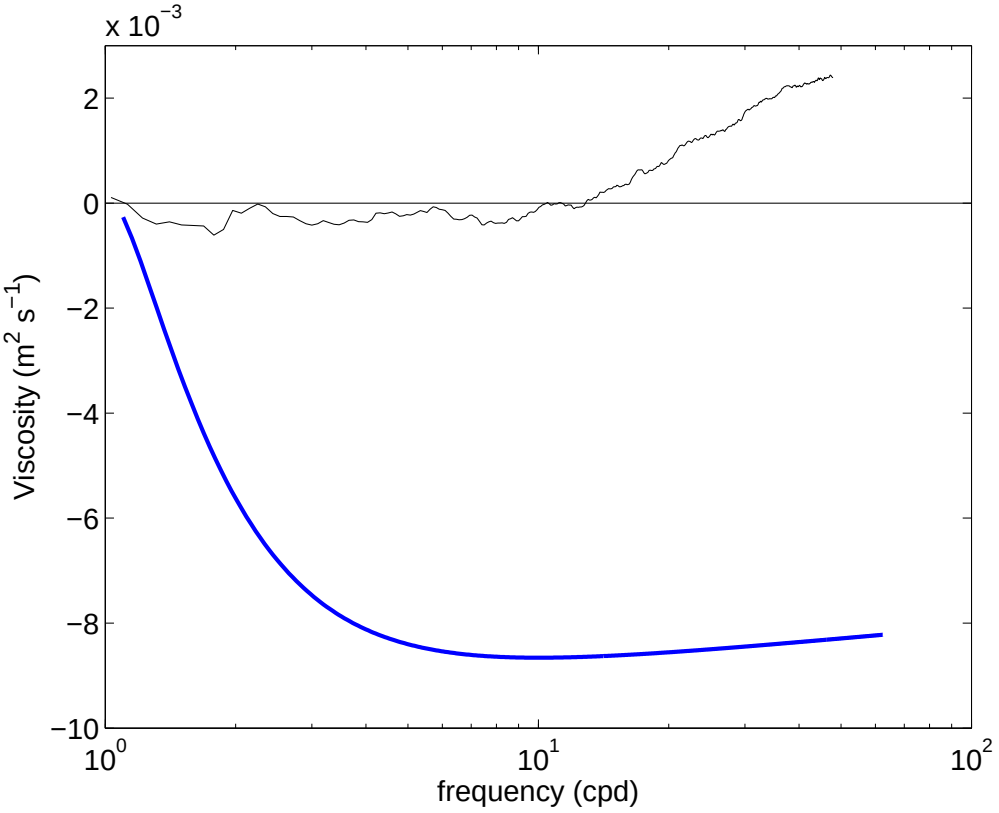

FIG. 4. Cumulative integrals of the spectral function $-sgn(\overline{u}_z)[C_{u''w''} - fC_{v''b''}/N^2]/(\overline{u}_z^2)^{1/2} - sgn(\overline{v}_z)[C_{v''w''} + fC_{u''b''}/N^2]/(\overline{v}_z^2)^{1/2}$, to provide estimates of the vertical viscosity $(\nu_v + \frac{f^2}{N^2}K_h)$. Over plotted as a thick line is a GM76 based estimate for the corresponding viscosity estimate (28).

List of Tables

TABLE 1. Moments of the kinetic energy spectrum, (29). Column two contains the observed estimates, column three the moment representation of the first difference estimates and the fourth "fully resolved" estimates of the moments integrated to "dissipation scale" of $\frac{2\pi}{k_h^c} = 10$ km .

variable	observed	estimated	"fully resolved"
E_k	4.0×10^{-3} m^2 s^{-2}		4.0×10^{-3} m^2 s^{-2}
$2\nu\zeta^2$	3.0×10^{-10} W/kg	3.9×10^{-10} W/kg	4.6×10^{-10} W/kg
ζ^2	3.5×10^{-12} s^{-2}	3.9×10^{-12} s^{-2}	7.0×10^{-12} s^{-2}
$\mid \nabla_h \zeta \mid^2$	6.7×10^{-21} m^{-2} s^{-2}	1.3×10^{-20} m^{-2} s^{-2}	3.8×10^{-19} m^{-2} s^{-2}
$\frac{1}{2}\nu \mid \nabla_h \zeta \mid^2$	1.7×10^{-19} s^{-3}	3.3×10^{-19} s^{-3}	1.2×10^{-18} s^{-3}